Fission Yeast Myosin-I, Myo1p, Stimulates Actin Assembly by Arp2/3 Complex and Shares Functions with WASp

Wei-Lih Lee,*‡ Magdalena Bezanilla,‡ and Thomas D. Pollard‡

*Graduate Program in Biochemistry, Cellular and Molecular Biology, Johns Hopkins University School of Medicine, Baltimore, Maryland 21205; and ‡Structural Biology Laboratory, The Salk Institute for Biological Studies, La Jolla, California 92037

Abstract. Fission yeast *myo1*$^+$ encodes a myosin-I with all three tail homology domains (TH1, 2, 3) found in typical long-tailed myosin-Is. Myo1p tail also contains a COOH-terminal acidic region similar to the A-domain of WASp/Scar proteins and other fungal myosin-Is. Our analysis shows that Myo1p and Wsp1p, the fission yeast WASp-like protein, share functions and cooperate in controlling actin assembly. First, Myo1p localizes to cortical patches enriched at tips of growing cells and at sites of cell division. Myo1p patches partially colocalize with actin patches and are dependent on an intact actin cytoskeleton. Second, although deletion of *myo1*$^+$ is not lethal, *Δmyo1* cells have actin cytoskeletal defects, including loss of polarized cell growth, delocalized actin patches, and mating defects. Third, additional disruption of *wsp1*$^+$ is synthetically lethal, suggesting that these genes may share functions. In mapping the domains of Myo1p tail that share function with Wsp1p, we discovered that a Myo1p construct with just the head and TH1 domains is sufficient for cortical localization and to rescue all *Δmyo1* defects. However, it fails to rescue the *Δmyo1 Δwsp1* lethality. Additional tail domains, TH2 and TH3, are required to complement the double mutant. Fourth, we show that a recombinant Myo1p tail binds to Arp2/3 complex and activates its actin nucleation activity.

Key words: fission yeast • myosin-I • WASp • Arp2/3 complex • actin assembly

Introduction

Myosin-I is an actin-dependent membrane-based molecular motor. Many organisms express multiple myosin-Is with similar catalytic domains but different tails containing binding sites for membrane lipids and a variety of proteins. These tail-ligand interactions are postulated to target myosin-I isoforms to various intracellular locations and/or to adapt them to different actin-dependent processes such as motility, endocytosis, phagocytosis and polarized cell growth (Doberstein et al., 1993; Baines et al., 1995; McGoldrick et al., 1995; Goodson et al., 1996). Identifying the tail ligands and understanding the significance of the tail-ligand interactions have been the object of much study in several different organisms.

The catalytic domain of all myosin-Is is followed by a region with one to five light-chain binding (IQ)[1] motifs, and a basic tail domain called tail homology 1 (TH1) that binds acidic phospholipids (Doberstein and Pollard, 1992) and actin filaments (Lee et al., 1999). In addition to TH1, long-tailed myosin-Is contain a Gly/Pro/Ala-rich TH2 domain and an *src* homology 3 domain called TH3. TH2 also binds actin filaments (Jung and Hammer, 1994; Rosenfeld and Rener, 1994) and TH3 mediates interactions with adaptor proteins.

The COOH terminus of WASp/Scar proteins, containing an acidic A-domain, stimulates actin assembly by interacting with Arp2/3 complex. In animal cells, WASp/Scar proteins provide a link to signaling molecules affecting the actin cytoskeleton (reviewed by Higgs and Pollard, 1999). Interestingly, budding yeast myosin-I tails also bind Arp2/3 complex via a WASp-like A-domain at their COOH termini (Evangelista et al., 2000; Lechler et al., 2000). Deletions of A-domains from the yeast WASp/Scar homologue, Bee1p/Las17p, and myosin-Is led to drastic growth and actin organization defects (Evangelista et al., 2000; Lechler et al., 2000). Although data was not presented showing activation of Arp2/3 complex, these results implicated budding yeast myosin-Is in Bee1p-stimulated and Arp2/3 complex-mediated actin assembly.

Before any knowledge of this work on budding yeast myosin-Is, we identified a WASp-like acidic A-domain at the COOH terminus of Myo1p, a myosin-I from *Schizosac-*

The online version of this article contains supplemental material.

Address correspondence to Thomas D. Pollard, The Salk Institute for Biological Studies, 10010 North Torrey Pines Rd., La Jolla, CA 92037. Tel.: (858) 453-4100, ext. 1716. Fax: (858) 452-3683. E-mail: pollard@salk.edu

[1]*Abbreviations used in this paper:* EMM, Edinburgh minimal media; GFP, green fluorescent protein; IQ motif, light-chain binding motif; TH, tail homology.

charomyces pombe. Here we show with quantitative assays that Myo1p tail binds to and stimulates nucleation activity of Arp2/3 complex. Consistent with a role in regulating the actin cytoskeleton, disruption of *myo1*$^+$ causes abnormal morphology due to depolarization of actin patches. Unlike budding yeast and other known long-tailed myosin-Is, all defects associated with loss of Myo1p were rescued by a construct containing only the head and TH1 domain. This construct was also sufficient for localization to cortical patches. Although deletion of *myo1*$^+$ is not lethal, additional disruption of the COOH terminus of Wsp1p, a fission yeast WASp homologue, results in synthetic lethality. Myo1p, Wsp1p, or Myo1p lacking the A-domain rescues this lethality. This differs from budding yeast, where deletion of A-domains from WASp and myosin-I resulted in severe growth defects. Interestingly, Myo1p lacking the TH3 and A-domains, a construct that fully complements loss of Myo1p, fails to rescue the absence of both A-domains from Wsp1p and Myo1p, implicating the TH3 domain in myosin-I–mediated Arp2/3 complex activation in fission yeast. Our results suggest that in cooperation with Wsp1p, Myo1p directly regulates actin assembly.

Materials and Methods

Strains, Media, and Transformation

Table I lists the *S. pombe* strains used in this study. Fission yeast culture and genetic manipulations were carried out by standard methods. Transformation of *S. pombe* was achieved by electroporation (Moreno et al., 1991).

Identification and Cloning of *myo1*$^+$ and *wsp1*$^+$

Three uncharacterized myosin heavy chain genes in the Sanger database were identified by blasting (Altschul et al., 1990) with the catalytic domain sequence of *Acanthamoeba* myosin-IA. Phylogenetic analyses (Lee et al., 1999) of these new myosin sequences established the one in cosmid SPBC146 is a type-I myosin gene, and the two in SPBC2D10 and SPCC1919 are type-V myosin genes, so we named them *myo1*$^+$, *myo5*$^+$, and *myp5*$^+$.

We cloned a 5-kb EcoRI fragment containing the *myo1*$^+$ locus from SPBC146 into pBluescript. This construct is pBSmyo1. Total RNA from mid-log wild-type cells was amplified by 5′-RACE PCR (Life Technologies) and the products were subcloned and sequenced.

We identified a WASp-like gene in cosmid SPAC4F10. This *wsp1*$^+$ gene was previously submitted to Genbank (GenBank/EMBL/DDBJ accession number AAB92587). We identified exons in *wsp1*$^+$ by comparing its sequence with other WASp sequences and searching for the usually conserved 5′ (GTAC) and 3′ (CCAG) splice sites. We amplified a 3-kb fragment containing the entire *wsp1*$^+$ locus from genomic DNA, cloned it into pBluescript, and sequenced it. This construct is pBSwsp1.

Construction of *myo1*$^+$ or *wsp1*$^+$ Disruption Strains

Integration of linear *myo1*$^+$ and *wsp1*$^+$ disruption constructs (see Figs. 1 A and 6 A) into *his3-D1* or *leu1-32* wild-type diploid cells was screened by PCR. Stable transformed diploids were sporulated on malt extract and individual spores were dissected from tetrads and germinated on Yeast Extract Supplemented (YES). In either disruption, four viable spores were obtained, of which two were His$^+$ or Leu$^+$ containing the disrupted allele. We verified disruptions in viable haploids by PCR and Southern blot. Disruption of *wsp1*$^+$ allows expression of only the NH_2-terminal 346 residues, since an in-frame stop codon was created at the 5′ ligation site of the leu$^+$ insert.

The *myo1*$^+$ locus is flanked 5′ by a coatomer beta subunit gene and 3′ closely by a ubiquinone biosynthesis monooxygenase gene. The coatomer beta subunit gene has the same transcriptional orientation as *myo1*$^+$, but the ubiquinone monooxygenase gene is in opposite orientation. Disruption of *myo1*$^+$ by removing an NdeI-SalI fragment was lethal and could not be rescued by transforming plasmids carrying full-length *myo1*$^+$ gene (pUR-myo1 or pSGP-myo1). This NdeI-SalI fragment includes sequences coding for residues 249–1217 and 179 bp of 3′ untranslated region of *myo1*$^+$ gene, leaving the open reading frame of the downstream ubiquinone monooxygenase gene intact. Since we were unable to rescue this *myo1*$^+$ disruption with complementing plasmids, we concluded that the function of the downstream ubiquinone monooxygenase gene was most likely affected, perhaps at the level of transcript stability.

Construction of Expression and Complementation Constructs

We used sequences of other myosin-Is for which tail domains have been defined proteolytically (Lynch et al., 1986; Lee et al., 1999) to determine the boundaries between TH1, 2, 3, and A-domains of Myo1p: head consisted of residues 1–771; TH1, 772–966; TH2, 967–1112; TH3, 1113–1163; A, 1164–1217. To express full-length Myo1p with green fluorescent protein (GFP) fused to its NH_2 terminus, GFP-H/1/2/3/A, an engineered NotI-SalI fragment containing *myo1*$^+$ without the ATG and intron was cloned into NotI- and SalI-digested pSGP573, a GFP-tagging vector that carries the thiamine-repressible *nmt1*$^+$ promoter and the *ura4*$^+$ marker (Pasion and Forsburg, 1999). GFP-1, GFP-2/3/A, and GFP-1/2/3/A were made similarly in pSGP573 using primer sets that annealed to corresponding domains. We replaced a BamHI-SalI fragment coding the whole tail in GFP-H/1/2/3/A with one containing just TH1 for GFP-H/1. We removed this BamHI-SalI fragment for GFP-H, but this construction resulted in 62 non-Myo1p residues COOH-terminal to GFP-H. To test for complementation and overexpression, Ura$^+$ transformants were selected and streaked to permissive and nonpermissive conditions ±15 μM thiamine.

We made constructs expressing mutant Myo1p with COOH-terminal deletions designed to integrate at the *puc1*$^+$ locus. We cloned a NotI fragment containing *S. pombe puc1*$^+$ (Forsburg and Nurse, 1991) into NotI-digested pJK210 (Keeney and Boeke, 1994), a pBluescript plasmid containing only the *ura4*$^+$ marker. The resulting vector is pJK-puc1. We then subcloned *myo1*$^+$ into pJK-puc1 at a unique EcoRI site for H/1/2/3/A. We replaced a BamHI fragment coding the whole tail in H/1/2/3/A with TH1, TH1/2, and TH1/2/3 fragments amplified using appropriate primer sets for H/1 (residues 1–966), H/1/2 (residues 1–1112), and H/1/2/3 (residues 1–1163). We made H (residues 1–786) by removing the whole BamHI fragment in H/1/2/3/A, but this resulted in 10 non-Myo1p residues COOH-terminal to the head domain. To test for complementation, *Δmyo1* cells were transformed with these integrating constructs linearized

Table I. Strains Used in this Study

Strain	Genotype
FY527	*h*$^-$ *his3-D1 leu1-32 ura4-D18 ade6-M216*
FY528	*h*$^+$ *his3-D1 leu1-32 ura4-D18 ade6-M210*
FY436	*h*$^-$ *his7-366 ura4-D18 leu1-32 ade6-M216*
TP135	*h*$^-$ *Δmyo1::his3*$^+$ *his3-D1 leu1-32 ura4-D18 ade6-M216*
TP137	*h*$^-$ *Δmyo1::his3*$^+$ *puc1*$^+$*::[pUP-myo1 ura4*$^+$*] his3-D1 leu1-32 ura4-D18 ade6-M216*
TP138	*h*$^-$ *Δmyo1::his3*$^+$ *puc1*$^+$*::[pUP ura4*$^+$*] his3-D1 leu1-32 ura4-D18 ade6-M216*
TP139	*h*$^-$ *Δmyo1::his3*$^+$ *puc1*$^+$*::[pUP-myo1Δ123A ura4*$^+$*] his3-D1 leu1-32 ura4-D18 ade6-M216*
TP140	*h*$^-$ *Δmyo1::his3*$^+$ *puc1*$^+$*::[pUP-myo1Δ23A ura4*$^+$*] his3-D1 leu1-32 ura4-D18 ade6-M216*
TP141	*h*$^-$ *Δmyo1::his3*$^+$ *puc1*$^+$*::[pUP-myo1Δ3A ura4*$^+$*] his3-D1 leu1-32 ura4-D18 ade6-M216*
TP142	*h*$^-$ *Δmyo1::his3*$^+$ *puc1*$^+$*::[pUP-myo1ΔA ura4*$^+$*] his3-D1 leu1-32 ura4-D18 ade6-M216*
TP145	*h*$^+$ *Δwsp1::leu1*$^+$ *his3-D1 leu1-32 ura4-D18 ade6-M210*

by XhoI in the middle of the *puc1*$^+$. Stable Ura$^+$ transformants were selected and streaked to permissive and nonpermissive conditions.

pUR19-wsp1 was made by subcloning *wsp1*$^+$ from pBSwsp1 into a unique EcoRI site in pUR19, an ars1-containing fission yeast vector that carries the *ura4*$^+$ marker (Barbet et al., 1992). To identify strains carrying *ura4*$^+$-marked *wsp1*$^+$ in the background of *ura4*$^+$-marked Myo1p mutants, we made pUR-wsp1/Kan^r by subcloning a SalI-SacI fragment containing the kanamycin resistance gene from pFA6a (Wach et al., 1994) into SalI- and SacI-digested pUR19-wsp1. All constructs above were verified by sequencing.

Microscopy

Cells were stained with calcofluor (Balasubramanian et al., 1997) and with rhodamine-phalloidin by modification of a published procedure (Balasubramanian et al., 1997). Incubation with rhodamine-phalloidin for 30 min at 24°C and washing with 1 ml PBS improved staining. For actin disruption experiments, cells were treated with 100 μM latrunculin-A dissolved in DMSO or with the same volume of DMSO. After a 20-min incubation at 32°C, cells were fixed and stained for actin as

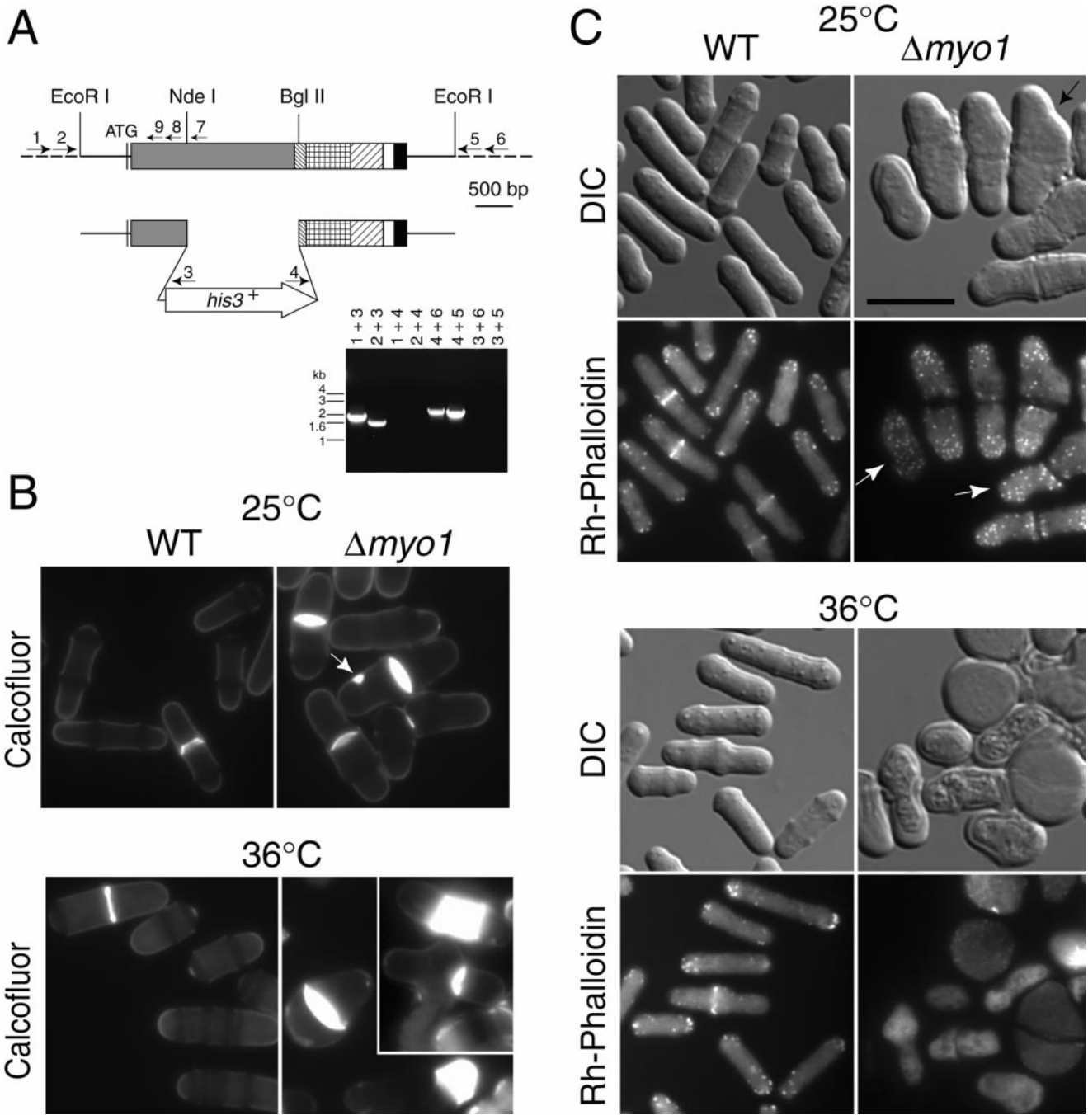

Figure 1. Targeted disruption of *myo1*$^+$. (A) Scale drawing of the *myo1*$^+$ locus. Sequences coding the domains of Myo1p are filled with different patterns. Dashed lines indicate sequences outside the disruption construct, which is shown below the locus. *myo1*$^+$ was disrupted in a *his3*$^-$ diploid strain by replacing an NdeI–BglII fragment with the *his3*$^+$ gene. The gel shows PCR amplification of the genomic locus from His$^+$ diploids disrupted in one of the two *myo1*$^+$ loci. Primers used for amplification are indicated as small arrows, and are indicated above each lane of the agarose gel. (B–C) Wild-type and *Δmyo1* cells grown to log phase in EMM-His at 25°C were shifted to 36°C for 5 h. Cells were stained before and after shifting with calcofluor (B) or rhodamine-phalloidin (C). Arrows indicate examples of aberrant cell morphology, mistargeting of cell-wall material, and actin abnormalities. Scale bar, 10 μm.

above. For localization studies, mid-log cells grown in 0.05 μM thiamine (Javerzat et al., 1996) were visualized directly or fixed in −80°C methanol. Cells were observed with a 100× objective on an IX70 microscope (Olympus) and images were collected on a digital CCD camera (Hamamatsu). Deconvolution microscopy was performed as described (Bezanilla et al., 2000).

Actin Polymerization and Binding Assays

Actin was purified from rabbit skeletal muscle (Spudich and Watt, 1971). Purified Arp2/3 complex was from *Acanthamoeba* and bovine thymus (Blanchoin et al., 2000). We subcloned TH2/3/A insert into the BamHI and EcoRI sites of pGex2T vector for bacterial expression. GST-2/3/A was purified on a glutathione-Sepharose column (Amersham Pharmacia Biotech), and dialyzed versus 10 mM Tris, pH 7, 65 mM NaCl, and 1 mM DTT. Actin polymerization (Higgs et al., 1999), glutathione bead copelleting, and actin filament copelleting assays (Lee et al., 1999) were as described. We measured actin polymerization lag and concentration of barbed ends as described (Pollard, 1986).

Table II. Fractions of Δmyo1, Δwsp1, and Wild-Type Cells with Normal or Abnormal Shape, with no Septum, One Septum, or Abnormal Septal Material

	Morphology		Cell wall by calcofluor staining		
	Normal rod	Abnormal shape	No septum	One septum	Abnormal septal material
	%	%	%	%	%
25°C					
wild-type	99.8	0.2	81.3	18.7	0
Δmyo1	84.0	16.0	49.3	37.0	13.7
36°C, 5 h					
wild-type	99.7	0.3	88.7	11.0	0.3
Δmyo1	48.0	52.0	24.0	19.7	56.3
32°C					
wild-type	99.7	0.3	91.7	8.3	0
Δwsp1	66.8	33.2	61.4	38.6	0

$n \geq 250$ cells in every case.

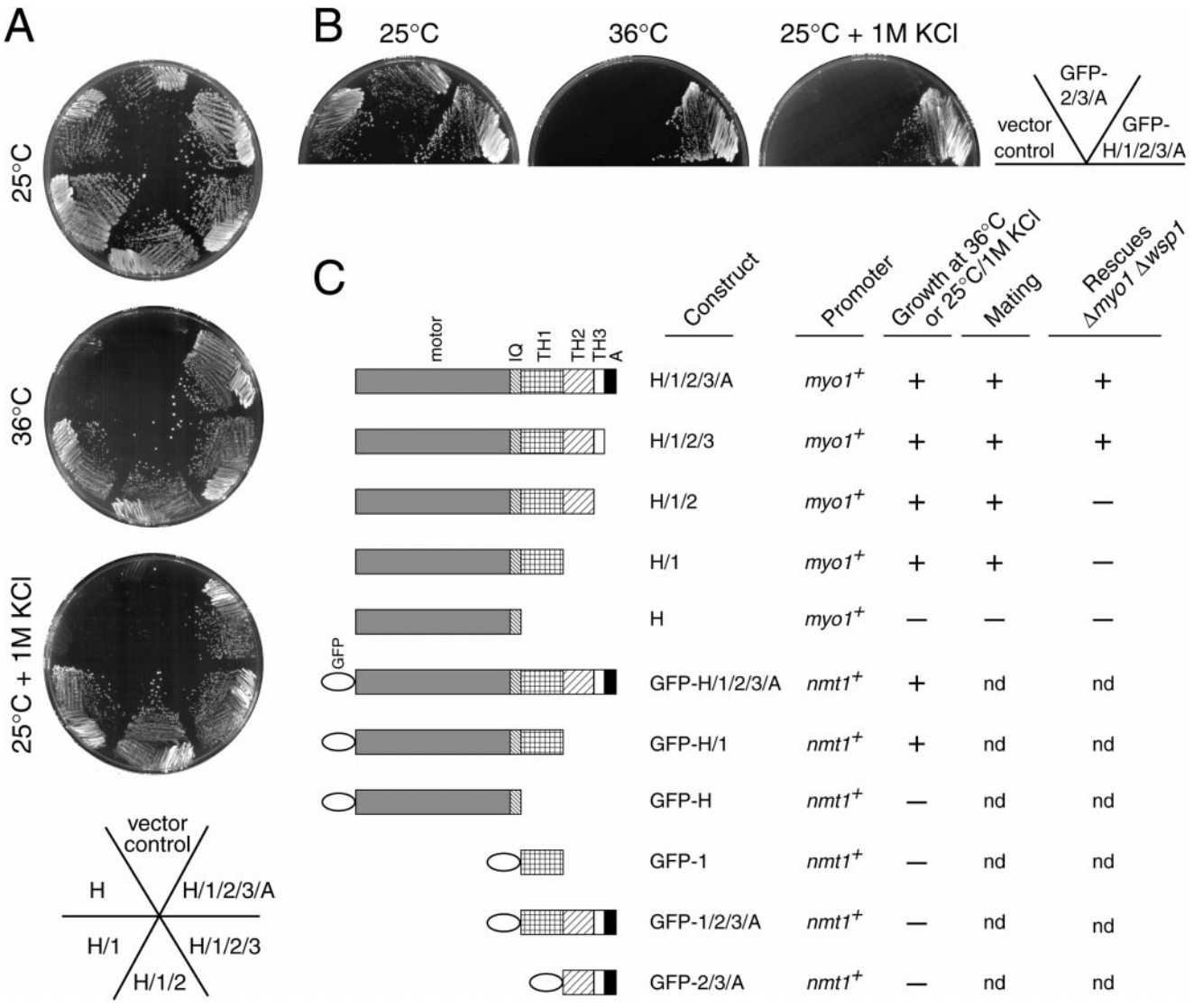

Figure 2. Complementation of temperature and salt sensitivities of *Δmyo1*. (A) *Δmyo1* cells transformed with integrated constructs: H/1/2/3/A, H/1/2/3, H/1/2, H/1, H, or pJK-puc1 (vector control). (B) *Δmyo1* cells transformed with GFP-H/1/2/3/A, GFP-2/3/A, or pSGP573 (vector control). All strains in A and B were streaked to EMM-Ura at 25°, 36°, or 25°C + 1 M KCl. (C) Schematic diagrams of constructs, the promoters controlling their expression, and their ability to rescue the temperature or salt sensitivity or mating defects of *Δmyo1*, and the lethality of *Δmyo1 Δwsp1*.

Online Supplemental Material

The online version of this article includes detailed methods used in constructing *myo1*$^+$ and *wsp1*$^+$ strains and two additional figures showing phylogenetic analysis of myosins, alignment of IQ motifs, 5′ RACE PCR of *myo1*$^+$ and latrunculin-A disruption of GFP-Myo1p patches. Available at http://www.jcb.org/cgi/content/full/151/4/789/DC1

Results

Identification of the myo1$^+$ *Gene*

As of August 2000, the *S. pombe* genome contained five genes with significant homology to *Acanthamoeba* myosin-IA catalytic domain. Of these five, two were previously characterized myosin-IIs called *myo2*$^+$ and *myp2*$^+$ (Bezanilla et al., 1997; Kitayama et al., 1997). We named the other myosin heavy chain genes *myo1*$^+$ (1,217 residues), *myo5*$^+$ (1,471 residues), and *myp5*$^+$ (1,516 residues). A phylogenetic tree built from sequence alignments of catalytic domains grouped *S. pombe* Myo1p with *Saccharomyces cerevisiae* myosin-Is (Myo3p and Myo5p) and *Aspergillus nidulans* MYOA with a bootstrapping value of 100% within the large myosin-I cluster (1,000 trials; see Figure S1 at http://www.jcb.org/cgi/content/full/151/4/789/DC1). In the same tree, *S. pombe* Myo5p and Myp5p joined *S. cerevisiae* (Myo2p and Myo4p), fly, chicken, and mouse myosin-Vs with a bootstrapping value of 100%. We conclude that *S. pombe* Myo1p is a myosin-I, and *S. pombe* Myo5p and Myp5p are myosin-Vs.

Myo1p and other known fungal myosin-Is have two similar IQ motifs, especially the first (Figure S1). Beyond the IQ motifs, Myo1p is a typical long-tailed myosin-I with the addition of a COOH-terminal A-domain. The basic TH1 domain has a calculated pI of 10. The TH2 domain is rich in Pro (20%), Ala (18%), Ser (12%), and Thr (11%). Abundant Ser and Thr in TH2 are unusual, found only in *S. cerevisiae* Myo3p and Myo5p, but not in other long-tailed myosin-Is. The A-domain is found on all fungal myosin-Is reported so far, but not on animal or protozoa myosin-Is. Two independent 5′-RACE products obtained from total *S. pombe* RNA using different sets of antisense and nested primers (Fig. 1 A, primers 7–9) established the presence of a 44-bp intron separating the ATG codon from the remaining coding sequence. *myo1*$^+$ transcript begins 43 bp upstream of the ATG.

Targeted Disruption of myo1$^+$

We disrupted *myo1*$^+$ by replacing >50% of the catalytic domain and the first IQ motif with the *his3*$^+$ gene (Fig. 1 A). This disruption allowed expression of only the NH_2-terminal 248 residues. Amplification with primers inside the *his3*$^+$ gene and primers outside the disruption construct verified that *myo1*$^+$ was disrupted in a His$^+$ diploid (Fig. 1 A, primers 1+3, 2+3, 4+6, and 4+5). All four progeny of this diploid were viable in YES at 25°C. Of these four colonies, two were His$^+$ (*Δmyo1*::*his3*$^+$) and always smaller in size. In liquid Edinburgh minimal media (EMM) at 25°C, *Δmyo1* cells grew with a doubling time of 12.5 h (n = 2) compared with 6.1 h (n = 4) for wild-type. These mid-log *Δmyo1* cells had aberrant morphology: 16% were round, slightly swollen, or irregularly shaped (Table II; Fig. 1 C); 13.7% had abnormal septal material

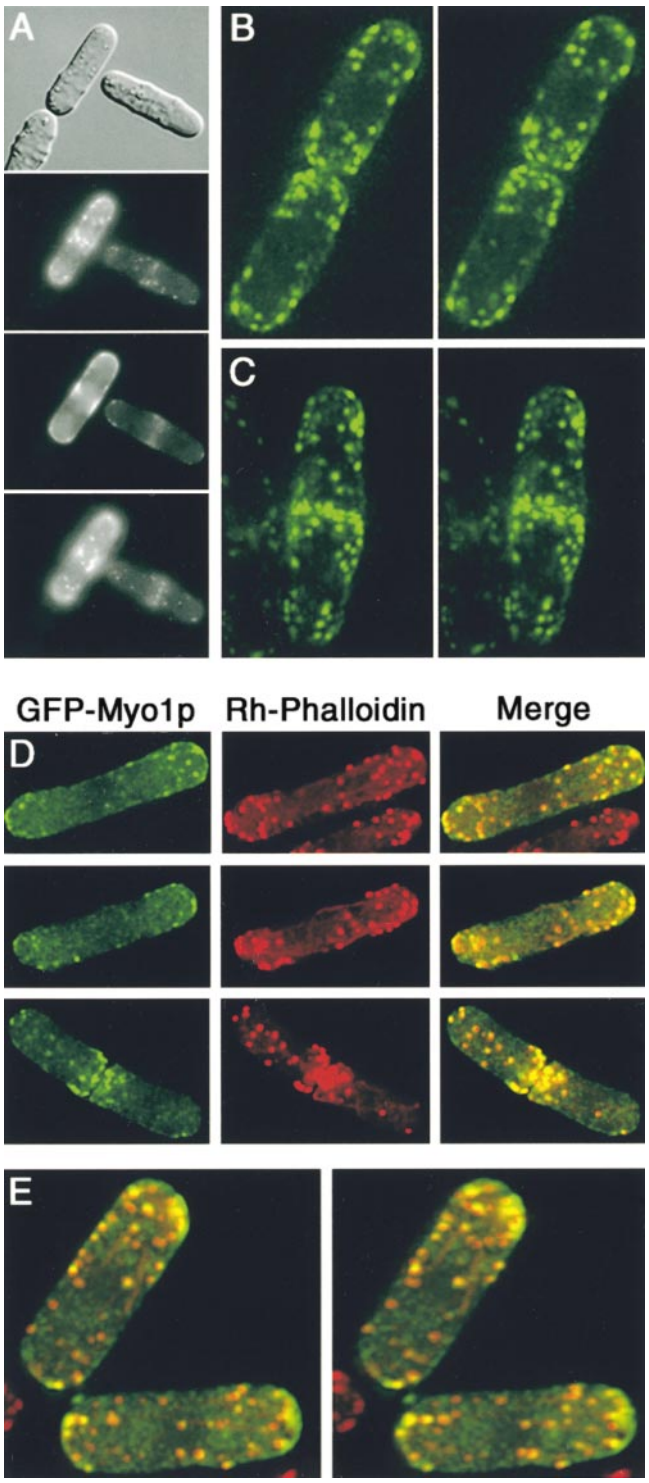

Figure 3. Localization of GFP-Myo1p in mid-log wild-type haploid cells. (A) Differential interference contrast and GFP-Myo1p fluorescence in live cells at three different focal planes. (B–C) Stereo pairs of three-dimensional reconstructions of live cells expressing GFP-Myo1p showing localization of Myo1p patches at cell periphery. (D–E) Colocalization of GFP-Myo1p and actin in fixed cells stained with rhodamine-phalloidin shown as full thickness stack of images from three-dimensional reconstructions (D) and as stereo pair (E). Images were obtained by a conventional fluorescence microscope (A) or a deconvolution Deltavision microscope (B–E).

(Fig. 1 B); and 37% had a septum, which was generally abnormally thick. Actin patches were delocalized in aberrantly shaped *Δmyo1* cells (Fig. 1 C, arrow), but those with rod shapes usually had polarized actin patches at growing ends or an actin ring in the middle of dividing cells.

Δmyo1 cells failed to form colonies at 17°C, 36°C, or, in the presence of 1 M KCl, at 25°C, where they died swollen, branched, abnormally shaped, and lysed. This terminal phenotype developed within 5 h after shifting from 25° to 36°C (Fig. 1, B and C) or to 1 M KCl at 25°C (not shown) in liquid EMM-His. Less than 1% of wild-type cells had abnormal morphology under these conditions (Table II). Calcofluor staining revealed the most striking effects of *myo1*$^+$ deletion in cells shifted to 36°C. More than half of *Δmyo1* cells (Table II; Fig. 1 B) had severely thickened septa, and abnormal septal material at one end, on one side, or all around the cell. Even those *Δmyo1* cells with normal rod morphology often had abnormally placed septal material. At 36°C, *Δmyo1* cells with abnormal morphology had no actin patches (Fig. 1 C). Since DAPI stained the nuclei of these fixed cells (not shown), the absence of actin patches was not likely due to failure of rhodamine-phalloidin to penetrate the cell wall or plasma membrane. Wild-type cells maintained normal septal deposition and polarized actin patches at 36°C.

Mating was defective in *Δmyo1* cells. When crossed with wild-type cells of opposite mating type on malt extract agar, zygotes were rare. Iodine vapor also revealed same coloring as nonmated controls, indicating that *Δmyo1* mated very inefficiently.

Complementation of Δmyo1 Phenotypes and Localization of GFP-Myo1p

To evaluate the function of the tail domains of Myo1p, we integrated constructs expressing full-length Myo1p (H/1/2/3/A) or Myo1p with COOH-terminal deletions (H/1/2/3, H/1/2, H/1, and H) under control of the native *myo1*$^+$ promoter into *Δmyo1* cells. All constructs, except H, restored growth at 17° (not shown), 36°, and 25°C with 1 M KCl (Fig. 2 A). *Δmyo1* cells transformed with construct H were indistinguishable from cells transformed with empty vector. Similarly, all constructs, except H, rescued *Δmyo1* mating defects assessed by iodine vapor staining. Thus, the head plus TH1 are the minimum domains needed to complement the absence of functional *myo1*$^+$.

GFP-Myo1p and GFP-H/1 restored wild-type growth to *Δmyo1* cells at 36° or 25°C with 1 M KCl (Fig. 2, B and C), showing that the GFP tag did not interfere with function. In the presence of thiamine, where they were expressed at a low level, as verified by microscopy, transformants had near wild-type morphology and colony size. In contrast, GFP fusions of head or tail alone (GFP-H, GFP-1, GFP-1/2/3/A, and GFP-2/3/A) failed to complement *Δmyo1* defects.

Full-length GFP-Myo1p localized to patches in wild-type as well as *Δmyo1* cells. Three-dimensional reconstructions made by deconvolution microscopy showed that all GFP-Myo1p patches were located at the periphery of living cells (Fig. 3, B and C), so they appeared in different focal planes by conventional fluorescence microscopy (Fig. 3 A). Like actin patches, these Myo1p patches usually concentrated at both growing ends or in the middle of dividing cells, and were dynamic, since we observed them moving along the cell cortex. We found that GFP-Myo1p patches partially colocalized with actin patches (Fig. 3, D and E). Staining of GFP-Myo1p–expressing cells with rhodamine-phalloidin revealed that ~25% of patches contained only GFP-Myo1p (green patches) and ~15% contained only actin (red patches). Approximately 60% of patches contained a variable ratio of actin and GFP-Myo1p, since these patches ranged in color from yellow to orange (350 patches counted). Latrunculin-A reversibly dispersed GFP-Myo1p from patches to a diffuse cytoplasmic fluorescence, indicating that cortical localization of

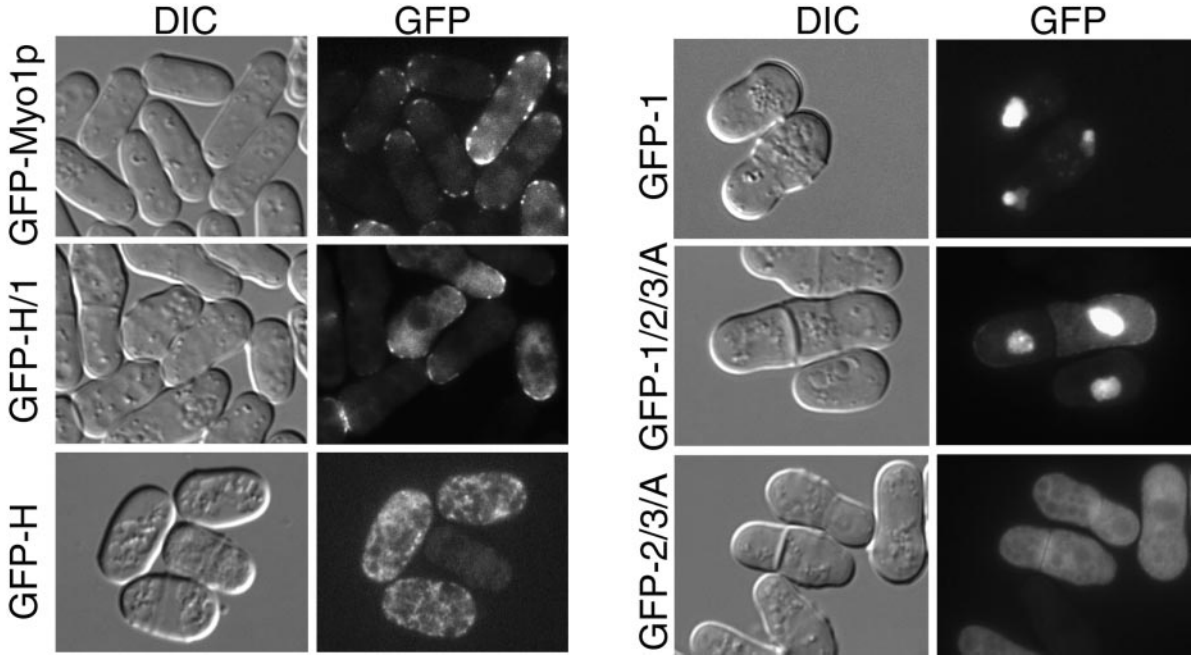

Figure 4. Localization of Myo1p head and/or tail constructs fused to GFP. Live mid-log cells expressing indicated constructs at 25°C in *Δmyo1* cells. All images were obtained by a conventional fluorescence microscope.

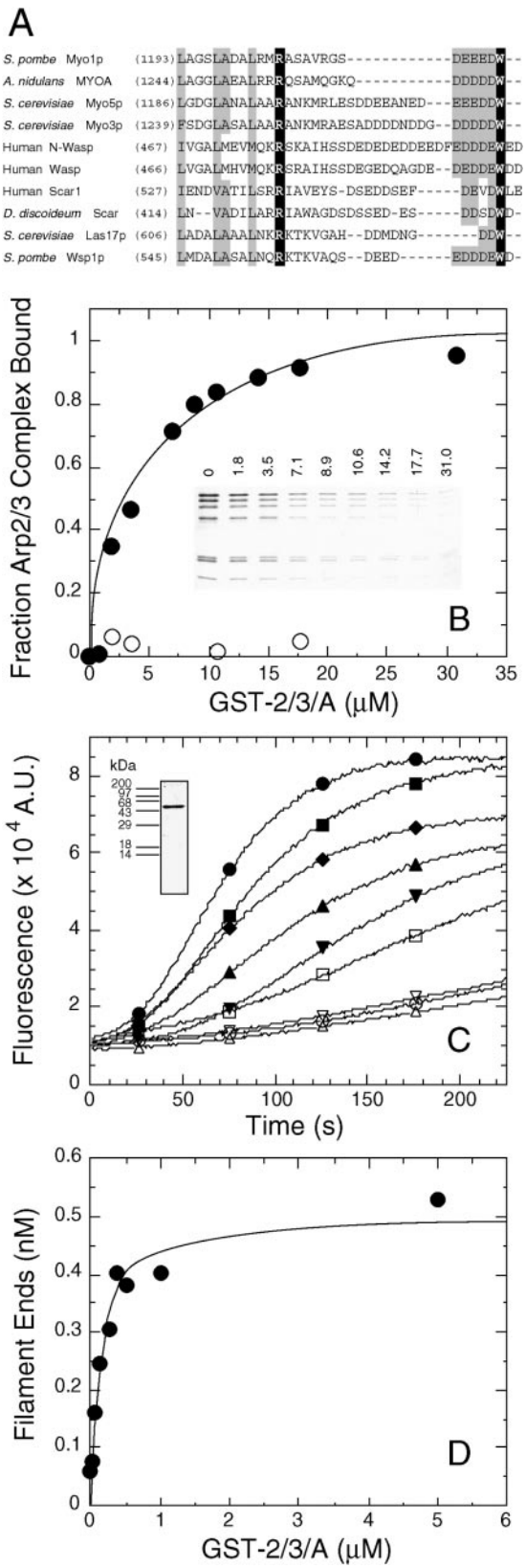

Figure 5. Activation of actin nucleation by Arp2/3 complex by Myo1p TH2/3/A. (A) Alignments of A-domains with WASp/Scar A-domains. Numbers in parentheses represent the starting residue in the alignment. Invariant and conserved residues are shaded black and gray. (B) Supernatant depletion assay for GST-2/3/A binding amoeba Arp2/3 complex. Conditions: GST-2/3/A immobilized on beads (●) was titrated into 0.3 μM amoeba Arp2/3 complex in 65 mM NaCl, 10 mM Tris, pH 7, 1 mM DTT. The same volumes of beads were the control (○). Beads were pelleted at 16,000 *g* and supernatant proteins were separated by SDS-PAGE, stained with Coomassie, and scanned to measure the fraction bound. The binding isotherm gives a K_d of ~5 μM. (Inset) Coomassie-stained gel of the supernatants showing Arp2/3 complex depletion. Numbers above each lane indicate total GST-2/3/A concentration on beads in micromolar. (C) Time course of polymerization of 4 μM monomeric Mg-ATP-actin (5% pyrene labeled). Conditions: 10 mM Tris, pH 7, 50 mM KCl, 1 mM $MgCl_2$, 1 mM EGTA, and 0.2 mM ATP. (▽) Actin alone, (△) actin with 50 nM amoeba Arp2/3 complex, (○) actin with 500 nM GST-2/3/A. Actin with 50 nM amoeba Arp2/3 complex and GST-2/3/A at concentrations of (nM): 63 (□), 125 (▼), 250 (▲), 375 (◆), 500 (■), and 5,000 (●). (Inset) SDS-PAGE of purified GST-2/3/A. (D) The concentration of filament ends produced by 50 nM amoeba Arp2/3 complex as a function of GST-2/3/A.

Myo1p depended on intact actin filaments. Expression levels from the *nmt1*$^+$ promoter varied from cell to cell, producing patches of different intensities but otherwise indistinguishable. Overexpression of GFP-Myo1p, while not toxic, produced uniform fluorescence throughout the cell periphery and large fluorescent aggregates in the cytoplasm. We conclude that expression of GFP-Myo1p at low levels mimics endogenous Myo1p localization.

GFP-H/1, a construct that rescued *Δmyo1* defects, localized to discrete patches similar to GFP-Myo1p in *Δmyo1* (Fig. 4) and wild-type cells. However, the level of expression was more variable from cell to cell and cytoplasmic fluorescence was greater for GFP-H/1 than for GFP-Myo1p. GFP fusions that failed to complement *Δmyo1* were either mislocalized to the nucleus (Fig. 4, GFP-1 and GFP-1/2/3/A), aggregated (GFP-H), or diffuse in the cytoplasm (GFP-2/3/A). Nuclear localization of GFP-1 and GFP-1/2/3/A were confirmed by staining with DAPI.

Myo1p Tail Binds and Activates Arp2/3 Complex

The sequence of Myo1p A-domain is similar to A-domains of WASp/Scar proteins that bind Arp2/3 complex (Fig. 5 A). Among known myosin tails, only fungal myosin-Is have A-domains. Two assays established that Myo1p tail interacts with Arp2/3 complex. In a supernatant depletion assay, purified amoeba Arp2/3 complex bound a fusion protein GST-2/3/A (GST fused to the NH_2 terminus of TH2/3/A-domains of Myo1p) immobilized on beads with a K_d of ~5 μM (Fig. 5 B). Control glutathione beads did not deplete Arp2/3 complex from the supernatant.

Purified GST-2/3/A stimulated actin filament nucleation by amoeba (Fig. 5 C) and bovine Arp2/3 complex (not shown). GST alone did not promote actin polymerization by Arp2/3 complex. Separately, neither GST-2/3/A nor the Arp2/3 complex had an appreciable effect on the time course of spontaneous polymerization, but together they reduced the lag at the outset of polymerization up to threefold (not shown) and generated ninefold more filament ends (Fig. 5 D). These effects plateaued at concentrations of GST-2/3/A > 1 μM. GST-2/3/A had lower affinity and activity than the GST-WA-domain of WASp (Higgs et al., 1999), perhaps due to using proteins from different species.

GST-2/3/A did not pellet with muscle actin filaments in actin polymerization buffer (not shown). Based on the concentrations used, the minimum value of the K_d for GST-2/3/A binding muscle actin filaments is 20 μM.

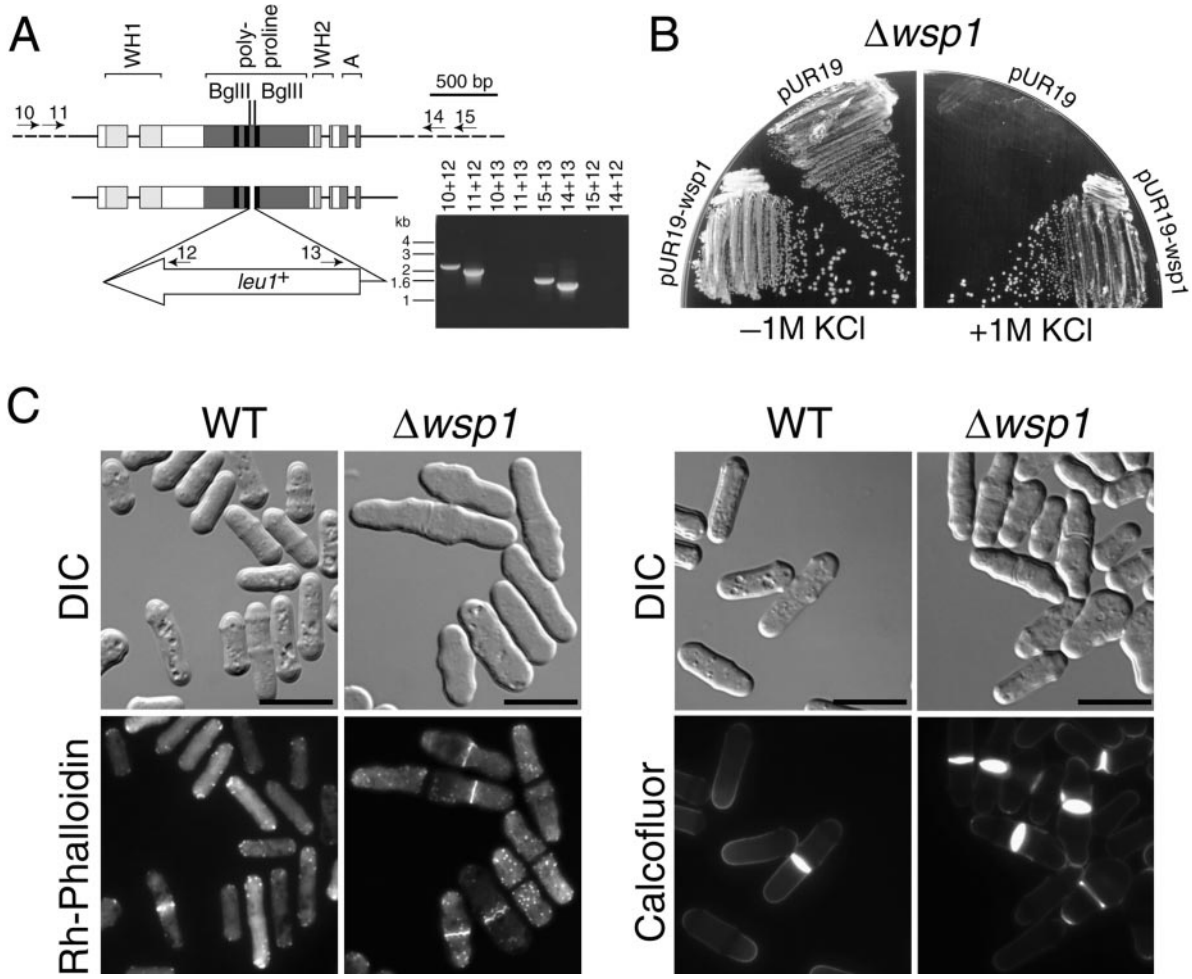

Figure 6. Targeted disruption of *wsp1*$^+$. (A) Scale drawing of the *wsp1*$^+$ locus showing exons (box) and introns (line). Sequences coding for various domains are filled with different shades. Black vertical bars within exon 2 indicate strings of six to seven proline residues. *wsp1*$^+$ was disrupted in a *leu1*$^-$ diploid by replacing a BglII–BglII fragment with an oppositely oriented *leu1*$^+$ gene. Agarose gel of PCR amplification from the disrupted locus of viable Leu$^+$ haploid is shown. (B) Viable Leu$^+$ haploids were transformed with plasmids and streaked on EMM-Leu ± 1 M KCl at 32°C. *Δwsp1* cells formed no colonies on 1 M KCl when transformed with an empty vector (pUR19), but were able to grow when transformed with a *wsp1*$^+$ genomic clone (pUR-wsp1). (C) Wild-type and *Δwsp1* cells grown to log phase in EMM-Leu at 32°C were stained with rhodamine-phalloidin and calcofluor. Scale bars, 10 μm.

Targeted Disruption of wsp1$^+$ *and Its Genetic Interaction with myo1*$^+$

We identified a WASp-like gene, *wsp1*$^+$, in the Sanger database as a potential activator of Arp2/3 complex. The genomic sequence of *wsp1*$^+$ has four exons encoding domains similar to WASp proteins: WH1 domain, a polyproline region, WH2 domain, and an acidic A-domain, but no GBD/CRIB sequence that might bind Cdc42p.

We made a *wsp1*$^+$ disruption strain (*Δwsp1*), which would produce a COOH-terminally truncated Wsp1p protein (Fig. 6 A). Tetrad dissection of individual asci and random spore analysis of a *Δwsp1*/*wsp1*$^+$ diploid revealed that COOH-terminal truncation of Wsp1p is not lethal. Amplification with specific primers from the genomic locus verified that *wsp1*$^+$ was disrupted in Leu$^+$ haploids (Fig. 6 A). *Δwsp1* cells formed smaller colonies than wild-type in selective EMM, were sensitive to 1 M KCl (Fig. 6 B) and mated inefficiently. A genomic clone of *wsp1*$^+$ (pUR19-wsp1) fully complemented the salt phenotype and mating defects. Like *Δmyo1* cells, *Δwsp1* cells had depolarized actin patches and morphological defects (Fig. 6 C). Disruption of *wsp1*$^+$ did not cause faulty targeting of septal material, but mid-log *Δwsp1* cells grown at 32°C did have more uniseptated cells than wild-type (Table II; Fig. 6 C). The lack of aberrant septal targeting suggests that, unlike Myo1p, Wsp1p is not involved in proper septal deposition.

To test for genetic interactions between *wsp1*$^+$ and *myo1*$^+$, we crossed *Δwsp1* with *Δmyo1* cells, by transforming each strain first with a complementing plasmid before mating (pUR-wsp1 for *Δwsp1*, pSGP573-myo1 for *Δmyo1*). The progeny from the cross were examined by random spore analysis after germination at 25°C. Marker analysis of 657 progeny indicated that wild-type (250, His$^-$, and Leu$^-$), *Δmyo1* (192 His$^+$), and *Δwsp1* (215 Leu$^+$) spores could be recovered. No spores carrying disruption of *myo1*$^+$ and *wsp1*$^+$ (0 His$^+$ and Leu$^+$) were recovered, so at the permissive temperature for both disruptions, *Δwsp1* is synthetically lethal with *Δmyo1*.

To test for functional redundancy between the tail of Myo1p and Wsp1p, we crossed *Δmyo1* cells containing integrated Myo1p mutants (H/1/2/3/A, H/1/2/3, H/1/2, H/1, and H) with *Δwsp1* cells carrying a modified pUR-wsp1. We

added the kanamycin resistance gene to pUR-wsp1 (= pUR-wsp1/Kan^r) to identify progeny carrying *ura4$^+$*-marked *wsp1$^+$* in the presence of *ura4$^+$*-marked Myo1p mutants. The progeny from these crosses were examined by random spore analysis after germination at 25°C in YES. We analyzed >400 progeny for each cross. Progeny carrying disruption of *myo1$^+$* and *wsp1$^+$* in the presence of integrated H/1/2/3/A or H/1/2/3 were recovered with expected mendelian segregation and independent of pUR-wsp1/Kan^r. H/1/2, H/1, or H progeny carrying both disruptions were always kanamycin resistant, indicating the presence of *wsp1$^+$*, and were recovered with significantly lower than expected frequency. We conclude that H/1/2/3/A and H/1/2/3, but not H/1/2, H/1 or H, rescue the lethality of *Δmyo1 Δwsp1*.

Discussion

Judging from the available sequence information (~95%) at the Sanger Genome Center, fission yeast potentially contains only one type-I myosin gene, making it attractive for detailed analysis of myosin-I functions. Multiple myosin-I genes in other organisms are interesting in terms of their specialized functions, but have been a burden experimentally in studies of basic functions.

Functions of Myo1p

Deletion of *myo1$^+$* causes defects in cell morphology and actin organization. Nonpermissive conditions greatly enhance these defects, leading to branched and rounded cells and eventually to cell death. Fission yeast cells grow in a polarized fashion, using the actin cytoskeleton to deliver essential materials to the growing ends of cells. The morphology of *Δmyo1* cells suggests that Myo1p has a role in regulating the sites of polarized growth, like the *S. pombe tea* and *orb* gene products (Verde et al., 1998). Interestingly, one of the round *orb* mutants, *orb2*, is the *pak1$^+$/shk1$^+$* gene (Verde et al., 1998), a member of the Ste20p/PAK family of kinases. As demonstrated in other organisms (Wu et al., 1997; Brzeska et al., 1989), Ste20p/PAK kinases activate myosin-I motor activity by phosphorylating a serine or threonine residue (TEDS rule site) in the catalytic domain. The TEDS rule site of Myo1p, Ser-361, may be a target of Pak1p/Shk1p, since disruption of *myo1$^+$* mimics the actin patch delocalization and rounded shape found in *orb2* mutant cells.

Consistent with a role in regulating polarized growth, Myo1p and Pak1p/Shk1p localize to growing ends. Localization of Myo1p depends on an intact actin cytoskeleton. However, not all Myo1p-containing patches are actin patches and not all actin patches contain Myo1p (Fig. 3, D and E). This intriguing observation indicates that there are distinct populations of patches that vary in molecular composition. If Myo1p is a target of Pak1p/Shk1p, it would be interesting to investigate whether these Myo1p-containing actin-deficient patches also contain Pak1p/Shk1p. Genetic interactions between *pak1$^+$/shk1$^+$* and *myo1$^+$*, phosphorylation of Myo1p by Pak1p/Shk1p, and localization of both proteins will be the subject of future work. We expect that Myo1p is part of a complicated and redundant system of proteins establishing polarity, since mutation in a variety of genes (for example, *tea*, *orb*, and now *wsp1$^+$*) clearly exhibit similar phenotypes.

Like Pak1p/Shk1p (Marcus et al., 1995; Ottilie et al., 1995), Myo1p is required for mating. Although the role of Myo1p in mating is not yet clear, it may again function downstream of Pak1p/Shk1p. In *S. cerevisiae*, a key regulator of PAK kinases, Cdc42p, localizes to the tip of α-factor–induced mating projections (Ziman et al., 1993). Given the conservation between budding and fission yeast Cdc42p (Miller and Johnson, 1994), we expect fission yeast Cdc42p to regulate Pak1p/Shk1p and thus Myo1p functions during conjugation.

Cells lacking Myo1p accumulate septal components abnormally, especially at high temperature (Fig. 1 B) and in high salt. Even under permissive conditions, most *Δmyo1* cells have a thick septum, and twice the number of *Δmyo1* cells have septa compared with wild-type. This function of Myo1p may be distinct from its role in maintaining cell shape, as many *Δmyo1* cells with normal rod morphology deposit cell wall abnormally. Thus, Myo1p may contribute to proper septation, perhaps transporting vesicles containing septal material to the division site.

Contribution of Myo1p Domains to Function

All known defects of *Δmyo1* cells are corrected by a construct with just the head and TH1 domains, a protein similar to a short-tailed myosin-I–like brush border myosin-I. This is surprising since important functions have been attributed to conserved parts of myosin-I tails that are missing in this construct: TH2 binds actin filaments (Jung and Hammer, 1994; Rosenfeld and Rener, 1994; Lee et al., 1999), TH3 binds adaptor proteins (Xu et al., 1995; Anderson et al., 1998), and A-domain interacts with Arp2/3 complex (Evangelista et al., 2000; Lechler et al., 2000). TH1 is essential for myosin-I function in fission yeast, since the H construct (with only the motor domain and IQ motifs) corrects no known defects of *Δmyo1* cells. The rest of the tail is not only unnecessary for function, but the tail does not even localize properly without the head.

Head and TH1 sequences are required and sufficient for proper localization of Myo1p. GFP-H/1 localizes like full-length Myo1p to cortical patches, but when expressed alone as a GFP-fusion protein, TH1 mislocalizes to the nucleus. TH1 contains many potential nuclear localization sequences, clusters of arginines and lysines, such as KKQRRR in the first 10 residues of this domain. Artifactual nuclear localization shows that associations of TH1 with acidic phospholipids and actin filaments are insufficient to prevent transport of a GFP-1 construct into the nucleus. The head, but not TH2/3/A, overcomes this nuclear targeting. This intriguing observation indicates that the motor domain of a myosin-I participates in targeting the protein in the cell. Similar work on mammalian myosin-Is (Ruppert et al., 1995; Durrbach et al., 1996) demonstrated that motor domain also contributes to localization in actin-rich cell surface structures like lamellipodia and membrane ruffles.

Role of Myo1p in Actin Assembly

The COOH-terminal A-domain of Myo1p is similar to the COOH-terminal A-domains of WASp/Scar proteins. Similar motifs on budding yeast myosin-Is and Bee1p/Las17p as well as other WASp proteins mediate physical interactions with Arp2/3 complex. In budding and fission yeasts,

ablation of Arp2/3 complex subunits is lethal or severely debilitating (Balasubramanian et al., 1996; Moreau et al., 1997). Purified Arp2/3 complex is intrinsically inactive in nucleating actin assembly, so it requires activation in the cell. We show here that a GST fusion protein containing the A-domain of Myo1p binds to and stimulates the nucleation activity of Arp2/3 complex. Our genetic results, however, show that this A-domain is not required for viability and Myo1p function, suggesting that myosin-I is not the only activator of Arp2/3 complex. Our findings provide evidence that Wsp1p is another essential activator of Arp2/3 complex. A *wsp1*$^+$ disruption that would produce a COOH-terminally truncated Wsp1p protein is not lethal, but this disruption leads to phenotypes similar to *Δmyo1* and is synthetically lethal with *Δmyo1*, indicating that these genes may share functions in regulating actin dynamics.

Interestingly, the minimal Myo1p construct for myosin-I function and localization, H/1, fails to rescue the *Δmyo1 Δwsp1* double-mutant lethality. Additional TH2 and TH3 domains are required to rescue the double-mutant, and rescued cells grow normally at 25°C in YES (data not shown). This differs from budding yeast, where deletion of A-domains from WASp and myosin-I result in severe growth defects. Our findings implicate TH3 domain in myosin-I–mediated activation of Arp2/3 complex in fission yeast, perhaps by recruiting an additional A-domain containing protein.

Function and Evolution of Myosin-I Tails

Work on other organisms has shown that tail domains are important for myosin-I function and localization, but the domains required appear to differ from organism to organism. In *S. cerevisiae*, a point mutation in TH3 or deletion of TH2 and TH3 domains disperses myosin-I–containing patches into diffuse cytoplasmic staining or alters the asymmetric distribution of patches to buds. These myosin-I mutants fail to complement defects of null cells (Anderson et al., 1998; Evangelista et al., 2000). In *Dictyostelium*, myoB lacking TH3 fails to rescue null phenotypes, but appears to localize properly (Novak and Titus, 1998). *Aspergillus nidulans* MYOA, on the other hand, does not require the TH3 domain, but deletion of TH1 or 30 residues rich in proline immediately COOH-terminal to TH3 results in a nonfunctional protein that does not localize properly (Yamashita et al., 2000). We find that TH1 is the crucial part of the tail in fission yeast Myo1p.

These functional differences in myosin-I tails may reflect a loss or gain of particular tail-ligand interactions subsequent to the divergence of these organisms during evolution. Phylogenetic analysis revealed that all myosin-I genes had a common ancestor in an early eukaryote more than one billion years ago. The sequences of their head domains distinguish them from other classes of myosin. On the other hand, analysis of their tail sequences suggested that myosin-I genes acquired their TH3 domains relatively late, in more than one independent event after the separation of contemporary organisms from their common ancestors (Lee et al., 1999). Thus, TH3 domains from various organisms would likely bind different ligands. This may explain why fission and budding yeast do not have a gene corresponding to *Acanthamoeba* Acan125 or *Dictyostelium* p116, proteins that bind the TH3 domains of amoeboid myosin-I tails. Also, acquisition of TH2 may also have been a relatively late and independent event, as suggested by the lack of alignment among TH2 sequences.

Addition of a COOH-terminal A-domain on fungal myosin-Is appears to have occurred once, soon after fungi diverged from animals and plants, ~800 million years ago. No known animal, plant, or protozoan myosin-Is has an A-domain. The A-domain on fungal myosin-Is was in place 550 million years ago when *S. pombe* diverged from the lineage giving rise to *S. cerevisiae* and *A. nidulans.* In fact, the four fungal myosin-Is are closely related throughout: the head sequences form a tight phylogenetically related cluster, the IQ motifs are similar, TH2 is abundant in serine and threonine (except MYOA), and all have an A-domain at their COOH termini (Figs. 5 A and S1, see supplemental material).

Since acquisition of the A-domain by fungal myosin-Is was a recent event, we hypothesize that other proteins may have also acquired A-domains late in their evolution. Similar acidic A-domain sequences are observed in various proteins not related to the WASp/Scar family or myosin-I, such as *S. cerevisiae* Abp1p and the intracellular domain of *Toxoplasma gondii* thrombospondin-related anonymous protiens (TRAP-related proteins). It would be interesting to investigate whether any of these A-domain–containing proteins may link nonfungal myosin-Is to Arp2/3 complex.

The authors thank Dr. Susan L. Forsburg for extensive advice and guidance on *S. pombe*. We thank Dr. David Ow for sharing his unpublished results on *wsp1*$^+$. We thank Harry Higgs and Don Kaiser for Arp2/3 complex, Laurent Blanchoin for input on actin filament disruption experiments, and Debbie T. Liang and other members of S.L. Forsburg laboratory for reagents and helpful suggestions.

This work was supported by National Institutes of Health research grant GM-26132 to T.D. Pollard.

Submitted: 19 June 2000
Revised: 12 September 2000
Accepted: 13 September 2000

References

Altschul, S.F., W. Gish, W. Miller, E.W. Myers, and D.J. Lipman. 1990. Basic local alignment search tool. *J. Mol. Biol.* 215:403–410.

Anderson, B.L., I. Boldogh, M. Evangelista, C. Boone, L.A. Greene, and L.A. Pon. 1998. The Src homology domain 3 (SH3) of a yeast type I myosin, Myo5p, binds to verprolin and is required for targeting to sites of actin polarization. *J. Cell Biol.* 141:1357–1370.

Baines, I.C., A. Corigliano-Murphy, and E.D. Korn. 1995. Quantification and localization of phosphorylated myosin I isoforms in *Acanthamoeba castellanii. J. Cell Biol.* 130:591–603.

Balasubramanian, M.K., A. Feoktistova, D. McCollum, and K.L. Gould. 1996. Fission yeast Sop2p: a novel and evolutionarily conserved protein that interacts with Arp3p and modulates profilin function. *EMBO (Eur. Mol. Biol. Organ.) J.* 15:6426–6437.

Balasubramanian, M.K., D. McCollum, and K.L. Gould. 1997. Cytokinesis in fission yeast *Schizosaccharomyces pombe. Methods Enzymol.* 283:494–506.

Barbet, N., W.J. Muriel, and A.M. Carr. 1992. Versatile shuttle vectors and genomic libraries for use with *Schizosaccharomyces pombe. Gene.* 114:59–66.

Bezanilla, M., S.L. Forsburg, and T.D. Pollard. 1997. Identification of a second Myosin-II in *Schizosaccharomyces pombe:* Myp2p is conditionally required for cytokinesis. *Mol. Biol. Cell.* 8:2693–2705.

Bezanilla, M., J.M. Wilson, and T.D. Pollard. 2000. Fission yeast myosin-II isoforms assemble into contractile rings at distinct times during mitosis. *Curr. Biol.* 10:397–400.

Blanchoin, L., K.J. Amann, H.N. Higgs, J.B. Marchand, D.A. Kaiser, and T.D. Pollard. 2000. Direct observation of dendritic actin filament networks nucleated by Arp2/3 complex and WASP/Scar proteins. *Nature.* 404:1007–1011.

Brzeska, H., T.J. Lynch, B. Martin, and E.D. Korn. 1989. The localization and sequence of the phosphorylation sites of *Acanthamoeba* myosins I. An improved method for locating the phosphorylated amino acid. *J. Biol. Chem.* 264:19340–19348.

Doberstein, S.K., I.C. Baines, G. Wiegand, E.D. Korn, and T.D. Pollard. 1993. Inhibition of contractile vacuole function in vivo by antibodies against myosin-I. *Nature.* 365:841–843.

Doberstein, S.K., and T.D. Pollard. 1992. Localization and specificity of the phospholipid and actin binding sites on the tail of *Acanthamoeba* myosin IC. *J. Cell Biol.* 117:1241–1249.

Durrbach, A., K. Collins, P. Matsudaira, D. Louvard, and E. Coudrier. 1996. Brush border myosin-I truncated in the motor domain impairs the distribution and the function of endocytic compartments in an hepatoma cell line. *Proc. Natl. Acad. Sci. USA*. 93:7053–7058.

Evangelista, M., B.M. Klebl, A.H. Tong, B.A. Webb, T. Leeuw, E. Leberer, M. Whiteway, D.Y. Thomas, and C. Boone. 2000. A role for myosin-I in actin assembly through interactions with Vrp1p, Bee1p, and the Arp2/3 complex. *J. Cell Biol.* 148:353–362.

Forsburg, S.L., and P. Nurse. 1991. Identification of a G1-type cyclin puc1$^+$ in the fission yeast *Schizosaccharomyces pombe* [published erratum appears in *Nature.* 1991. 352:648]. *Nature.* 351:245–248.

Goodson, H.V., B.L. Anderson, H.M. Warrick, L.A. Pon, and J.A. Spudich. 1996. Synthetic lethality screen identifies a novel yeast myosin I gene (MYO5): myosin I proteins are required for polarization of the actin cytoskeleton. *J. Cell Biol.* 133:1277–1291.

Higgs, H.N., L. Blanchoin, and T.D. Pollard. 1999. Influence of the C terminus of Wiskott-Aldrich syndrome protein (WASp) and the Arp2/3 complex on actin polymerization. *Biochemistry*. 38:15212–15222.

Higgs, H.N., and T.D. Pollard. 1999. Regulation of actin polymerization by Arp2/3 complex and WASp/Scar proteins. *J. Biol. Chem.* 274:32531–32534.

Javerzat, J.P., G. Cranston, and R.C. Allshire. 1996. Fission yeast genes which disrupt mitotic chromosome segregation when overexpressed. *Nucleic Acids Res.* 24:4676–4683.

Jung, G., and J.R. Hammer. 1994. The actin binding site in the tail domain of *Dictyostelium* myosin IC (myoC) resides within the glycine- and proline-rich sequence (tail homology region 2). *FEBS Lett.* 342:197–202.

Keeney, J.B., and J.D. Boeke. 1994. Efficient targeted integration at leu1-32 and ura4-294 in *Schizosaccharomyces pombe. Genetics.* 136:849–856.

Kitayama, C., A. Sugimoto, and M. Yamamoto. 1997. Type II myosin heavy chain encoded by the myo2 gene composes the contractile ring during cytokinesis in *Schizosaccharomyces pombe. J. Cell Biol.* 137:1309–1319.

Lechler, T., A. Shevchenko, and R. Li. 2000. Direct involvement of yeast type I myosins in Cdc42-dependent actin polymerization. *J. Cell Biol.* 148:363–373.

Lee, W.L., E.M. Ostap, H.G. Zot, and T.D. Pollard. 1999. Organization and ligand binding properties of the tail of *Acanthamoeba* myosin-IA. Identification of an actin-binding site in the basic (tail homology-1) domain. *J. Biol. Chem.* 274:35159–35171.

Lynch, T.J., J.P. Albanesi, E.D. Korn, E.A. Robinson, B. Bowers, and H. Fujisaki. 1986. ATPase activities and actin-binding properties of subfragments of *Acanthamoeba* myosin IA. *J. Biol. Chem.* 261:17156–17162.

Marcus, S., A. Polverino, E. Chang, D. Robbins, M.H. Cobb, and M.H. Wigler. 1995. Shk1, a homolog of the *Saccharomyces cerevisiae* Ste20 and mammalian p65PAK protein kinases, is a component of a Ras/Cdc42 signaling module in the fission yeast *Schizosaccharomyces pombe. Proc. Natl. Acad. Sci. USA.* 92:6180–6184.

McGoldrick, C.A., C. Gruver, and G.S. May. 1995. myoA of *Aspergillus nidulans* encodes an essential myosin I required for secretion and polarized growth. *J. Cell Biol.* 128:577–587.

Miller, P.J., and D.I. Johnson. 1994. Cdc42p GTPase is involved in controlling polarized cell growth in *Schizosaccharomyces pombe. Mol. Cell. Biol.* 14: 1075–1083.

Moreau, V., J.M. Galan, G. Devilliers, R. Haguenauer-Tsapis, and B. Winsor. 1997. The yeast actin-related protein Arp2p is required for the internalization step of endocytosis. *Mol. Biol. Cell.* 8:1361–1375.

Moreno, S., A. Klar, and P. Nurse. 1991. Molecular genetic analysis of fission yeast *Schizosaccharomyces pombe. Methods Enzymol.* 194:795–823.

Novak, K.D., and M.A. Titus. 1998. The myosin I SH3 domain and TEDS rule phosphorylation site are required for in vivo function. *Mol. Biol. Cell.* 9:75–88.

Ottilie, S., P.J. Miller, D.I. Johnson, C.L. Creasy, M.A. Sells, S. Bagrodia, S.L. Forsburg, and J. Chernoff. 1995. Fission yeast pak1$^+$ encodes a protein kinase that interacts with Cdc42p and is involved in the control of cell polarity and mating. *EMBO (Eur. Mol. Biol. Organ.) J.* 14:5908–5919.

Pasion, S.G., and S.L. Forsburg. 1999. Nuclear localization of *Schizosaccharomyces pombe* Mcm2/Cdc19p requires MCM complex assembly. *Mol. Biol. Cell.* 10:4043–4057.

Pollard, T.D. 1986. Rate constants for the reactions of ATP- and ADP-actin with the ends of actin filaments. *J. Cell Biol.* 103:2747–2754.

Rosenfeld, S.S., and B. Rener. 1994. The GPQ-rich segment of *Dictyostelium* myosin IB contains an actin binding site. *Biochemistry.* 33:2322–2328.

Ruppert, C., J. Godel, R.T. Muller, R. Kroschewski, J. Reinhard, and M. Bahler. 1995. Localization of the rat myosin I molecules myr 1 and myr 2 and in vivo targeting of their tail domains. *J. Cell Sci.* 108:3775–3786.

Spudich, J.A., and S. Watt. 1971. The regulation of rabbit skeletal muscle contraction. I. Biochemical studies of the interaction of the tropomyosin-troponin complex with actin and the proteolytic fragments of myosin. *J. Biol. Chem.* 246:4866–4871.

Verde, F., D.J. Wiley, and P. Nurse. 1998. Fission yeast orb6, a ser/thr protein kinase related to mammalian rho kinase and myotonic dystrophy kinase, is required for maintenance of cell polarity and coordinates cell morphogenesis with the cell cycle. *Proc. Natl. Acad. Sci. USA*. 95:7526–7531.

Wach, A., A. Brachat, R. Pohlmann, and P. Philippsen. 1994. New heterologous modules for classical or PCR-based gene disruptions in *Saccharomyces cerevisiae. Yeast.* 10:1793–1808.

Wu, C., V. Lytvyn, D.Y. Thomas, and E. Leberer. 1997. The phosphorylation site for Ste20p-like protein kinases is essential for the function of myosin-I in yeast. *J. Biol. Chem.* 272:30623–30626.

Xu, P., A.S. Zot, and H.G. Zot. 1995. Identification of Acan125 as a myosin-I-binding protein present with myosin-I on cellular organelles of *Acanthamoeba. J. Biol. Chem.* 270:25316–25319.

Yamashita, R.A., N. Osherov, and G.S. May. 2000. Localization of wild type and mutant class I myosin proteins in *Aspergillus nidulans* using GFP-fusion proteins. *Cell Motil. Cytoskelet.* 45:163–172.

Ziman, M., D. Preuss, J. Mulholland, J.M. O'Brien, D. Botstein, and D.I. Johnson. 1993. Subcellular localization of Cdc42p, a *Saccharomyces cerevisiae* GTP-binding protein involved in the control of cell polarity. *Mol. Biol. Cell.* 4:1307–1316.